INFLUENCE OF ANNEALING ON STRUCTURAL, ELECTRICAL AND GAS SENSING PROPERTIES OF THERMAL EVAPORATED NANOCRYSTALLINE ZNO THIN FILMS

U. D. Lad [1*], N. S. Kokode [2], U. J. Tupe [3]
[1,2]Research Centre in Physics, Department of Physics, N.H. College, Bramhapuri, Dist- Gadchiroli, India.
[3]Department of Electronic Science and Research Center, L.V.H College, Nashik, Dist- Nashik, India.

Abstract

In the field of gas sensor annealing temperature is a one of the most important factor, which influences structural property, crystallinity of material and gas sensing property of film. Hence, the present work elaborate effect of annealing on the structural, electrical and gas sensing properties of ZnO thin film developed by using thermal evaporation technique. ZnO thin films were prepared on alumina substrate. Prepared samples S2 and S3 were annealed at temperature 450ºC and 550ºC respectively in a muffle furnace for 2 hours. S1 is un-annealed prepared sample. The resistivity of the developed thin films increased with the increasing annealing temperature. Structural characterizations of thin films were studied using SEM, EDS and XRD standard tools. At a different ambient temperature and gases, gas sensing properties of ZnO thin films were investigated. The sample S3 exhibits more sensitivity of 87.47% at 150 ºC to NH_3 gas with sudden response (~ 09 sec) and recovery (~ 12 sec) time.

Keywords- *Annealing temperature, ZnO, Thin films, crystallinity, Sensitivity, PPM.*

I. INTRODUCTION:

For the past few decades, nanomaterials have played a vital role in the field of gas sensors (Baptista, 2018). The initial criteria of novel study of nanoparticles are the synthesis of the material. The development of systematic studies for the synthesis of metal oxide semiconductor nanoparticles is a current challenge synthetic procedures using bottom-up and top-down synthesis approach. Preparation of nanomaterials is a very important task hence; many researchers are using different synthesis methods like precipitation, co-precipitation, sol-gel, laser ablation, chemical vapour deposition, hydrothermal, and water–oil microemulsions, solvothermal, direct oxidation, electro deposition, sonochemical, microwave, colloidal, sputtering, ion beam and physical vapour deposition method. Physical vapour deposition method is also known as Physical vapour deposition transport (PVT). It mainly describes vacuum deposition methods (Baptista, 2018, Perrin, 2000).

On the basis of the thickness layer of deposited material on the substrate, films are broadly classified into two ways one is thick film and another is thin film. Generally the diameter of the thick film is in the range of 15 µm to 80 µm and the diameter of the thin film is in the range of 50 nm to 300 nm (Becker, 2001). Physical vapour deposition method is commonly used to prepare thin films. It describes a variety of vacuum deposition methods. In the physical vapour deposition method, phase of material changes from solid to a vapour and the phase again converted into solid at the time of preparation of thin film that is vapour condensation on the substrate. Substrate can be used as a glass or alumina. Sputtering and evaporation, these are the two common processes in physical vapour deposition (Shahidi, 2015, Yoke, 2015). The one of the most important advantages of the physical deposition method is for the preparation of the thin film chemical process is not involved. PVD method is very convenient and this method is applicable to prepare thin films of various types of materials. This method is also applicable to prepare the nanostructure of many metal oxide semiconductors. PVD method is classified into three types- a) ion sputtering b) thermal evaporation and C) arc discharge (Baptista, 2018, Yoke, 2015).

PVD technique is used in the different areas including mechanical for item manufacture, optical, electrical, chemical, for coating purpose, textile, firearms, solar panel, microscopy, medical/surgical, dental coating, industrial, jewellery and decorative purpose, fabrication of microelectronic devices, battery and fuel cell electrodes (Shahidi, 2015, Perrin,2000).

Zinc oxide (ZnO) is n-type metal-oxide semiconductor belongs to the XII column of periodic table and its atomic number is 30. It has a wider energy band gap 3.37eV and higher excitation binding energy. In the last few decades, ZnO has been used in various applications like solar cell, battery, display, optical, bioscience, photo detector, material science and gas sensor because of their excellent properties like less expensive, sensitivity and versatility (Becker, 2001, Corkery, 2013).

Ammonia (NH_3) gas is an air pollutant that is frequently found in industrial and livestock products. Ammonia with concentrations greater than 25 ppm is a toxic gas for humans and animals and prolonged exposure to NH_3 at unprotected levels can lead to lung disease in humans and animals, among other health problems (Corkery, 2013). NH_3 is characterized by nitrogen sources for soil fertilizers, neutral agents in the oil industry, gas refrigerants in industrial systems, and many uses in the pharmaceutical industry. Ammonia gas increases air pollution and it effect on health of public, the development of recent platforms for ammonia sensing at low temperature has attracted attention (Andre, 2018).

In the current research work, the effect of annealing temperature on the electrical, structural and gas sensing properties of ZnO nanocrystalline thin films have been studied.

II. EXPERIMENTAL WORK:

Preparation of ZnO thin films by thermal evaporated technique:

In this work, commercial nanocrystalline ZnO nano powder (99% purity) was used as the functional materials for preparing the ZnO thin film sensors. ZnO thin films were prepared by using thermal evaporated system. The system includes a conventional vacuum system, which was evacuated to 10^{-6} mbar by rotary and diffusion pump arrangement. The chamber was filled with vacuum and for deposition purpose alumina substrates were used. Before placing into the deposition chamber, the alumina substrates were cleaned using acetone and IR lamp. The substrates were placed 20-25 minutes under IR lamp. After that, ZnO powder place in molybdenum boat by some appropriate arrangement and using high voltage power supply, which was used as the target for evaporation. Then, prepared thin film samples of ZnO were annealed using muffle furnace at variation of two temperatures 450^{o}C and 550 ^{o}C for sample S2 and S3 respectively and used further study.

Characterizations of ZnO thin films:

Electrical characterizations of nanocrystalline ZnO thin films:

The electrical study were carried out by using following parameters –

1. Resistivity
2. Temperature coefficient of resistance (TCR) and
3. Activation energy at high temperature and low temperature region.

The resistivity, temperature coefficient of resistance (TCR) and activation energy was calculated using equations 1, 2 and 3 respectively.

$$\rho = \left(\frac{R \times b \times t}{l} \right) ohm - m \tag{2.1}$$

Where, t = thickness of the film sample, b = breadth of the thick film resistor in cm

$$TCR = \frac{1}{R_o}\left(\frac{\Delta R}{\Delta T} \right) /^{O} C \tag{2.2}$$

Where, ΔR = change in resistance between temperature T_1 and T_2, ΔT = temperature difference between T_1 and T_2 and R_o = Initial resistance of the film sample

$$R = R_o e^{-\Delta E/KT} \tag{2.3}$$

Where, R_o = the constant, ΔE = the activation energy of the electron transport in the conduction band (eV), K = Boltzman constant and T = Absolute temperature.

Structural characterizations of nanocrystalline ZnO thin films

The developed ZnO Nanocrystalline thin films were characterized by FESEM, EDS and XRD to study the surface morphology, elemental composition analysis and structural properties respectively. The thickness of the thin films was measured by using Taylor-Hobson (Taly-step UK) system. The thickness of the films was observed in the nm range.

Field Emission Scanning Electron Microscopy (SEM) {Model JOEL 6300 LA GERMANY} was utilized to characterize the surface morphology. The average particle size and diameter of nanoparticles were determined using Image-J software and SEM images of ZnO nanocrystalline thin films (Gao et al, 2000). The elemental analysis was carried out carried out using energy dispersive X-ray spectrometer EDAX (JOEL-2300, Germany). The specimen image can be obtained along with the elemental analysis of the selected area/features and distribution of selected elements.

The thin films low angle XRD was used X-ray generator [Miniflex Model, Japan] Rigaku diffractometer (DMAX-500) was employed. The XRD gives 2 Θ values which were used for identification of different phases and corresponding structure of the material present in the developed films. The obtained values are compared with Joint Committee on Powder Diffraction Standards (JCPDS) data files. The crystallite size (D) was calculated by Debye Scherer's formula equation 5 (Scarminio et al, 1997).

$$D = \frac{0.9\lambda}{\beta Cos\theta} \tag{2.4}$$

Where, β = Full angular width of diffraction peak at the at half maxima peak intensity,
λ =wavelength of X-radiation.

Gas sensing study of nanocrystalline ZnO thin films

The ammonia (NH_3) gas sensing properties were studied using static gas sensing system. Nanocrystalline ZnO thin films were used as sensing component. The resistance of the thin film was measured in an air atmosphere as well as in the presence of gas (at different ppm level) of interest at different operating temperatures. R_a is resistance of film in air and R_g is resistance of film in gas atmosphere. The resistance of thin film was measured by using half-bridge method. Figure 1 shows schematic diagram of electrical and gas sensing static system used in the current research work.

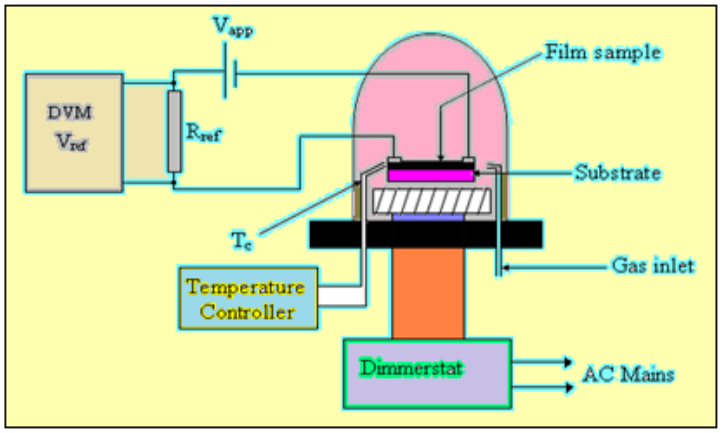

Fig. 1: Schematic diagram of electrical and gas sensing static system.

III. RESULT AND DISCUSSION:

Electrical Characterization:

Resistivity

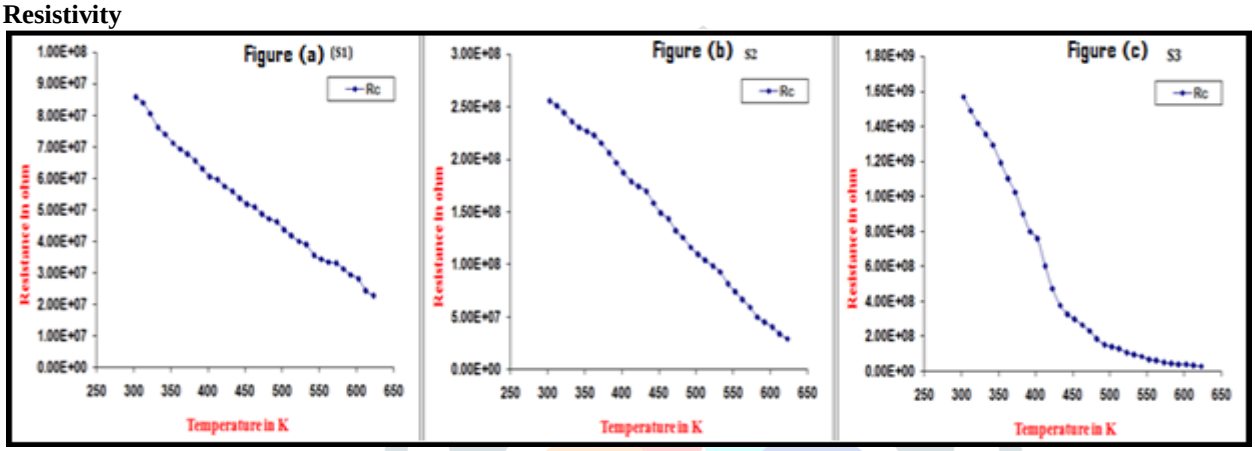

Fig. 2 (a) Resistance verses temperature of un-annealed thin film, (b) and (c) annealed thin films.

Figure 2 shows the variation of resistance S1, S2 and S3 samples with temperature for ZnO films. The DC resistance of ZnO thin films was measured by using half bridge method as a function of temperature. From figure, it clearly observed that resistance of the film decreases with temperature and decrease in resistance of film with increase in surrounding temperature indicate semiconductor behavior. It may be because the electrons receive enough energy to cross the barrier at the grain boundary, thus reducing the effective resistance of the thin film to a stable level at high temperatures (Rahman et al, 1997 and Fujihara, 2004). The resistivity of samples S1, S2 and S3 were calculated 1.8×10^{-4} Ω-cm, 5.6×10^{-3} Ω-cm and 3.6×10^{-1} Ω-cm respectively. As seen from result the resistivity was found highest to S3 sample. The resistivity of un-annealed S1 sample found very low as compare with S2 and S3 samples. The resistivity of the films increases with increasing annealing temperature of S2 and S3 samples. This can be attributed to the oxygen vacancies reduce because of increasing the annealing temperature in ZnO thin films, similar results have been reported Bouhssira, et al. (2006), Asghar et al. (2008) and Zaier , et. al. (2015) have reported similar results.

Activation energy

Figure 3 shows the plot is reversible in both heating and cooling cycles obeying the Arrhenius equation.

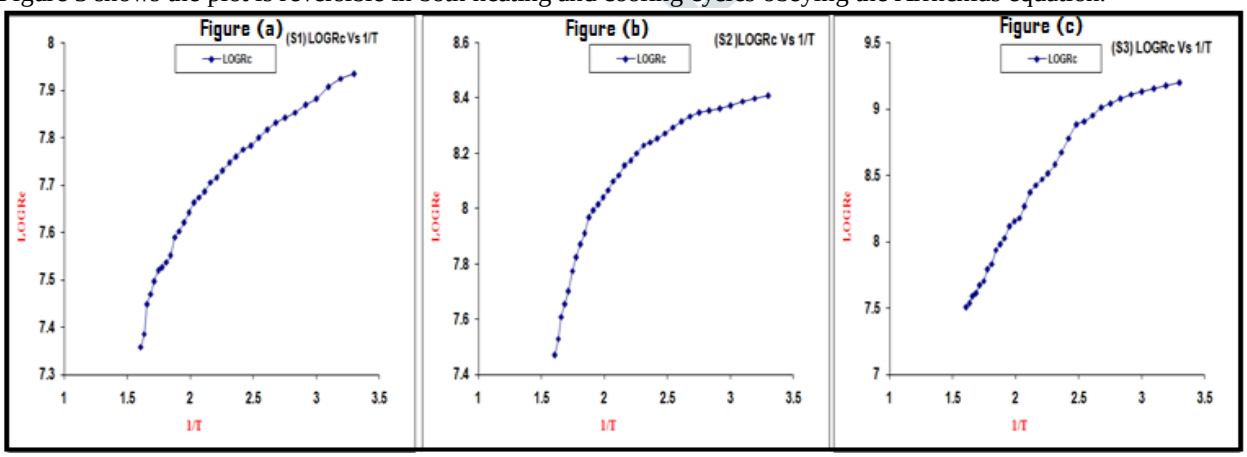

Fig. 3 (a) log R versus reciprocal of temperature of un-annealed thin film, (b) and (c) annealed thin films.

The activation energy of un-annealed S1 sample found very low as compare with S2 and S3 samples. The activation energy of the films increases with increasing annealing temperature of S2 and S3. Table 1 shows the activation energy of S1, S2 and S3 samples at high and low temperature region.

Temperature coefficient of resistance – TCR of ZnO thin films is calculated by using equation 3.

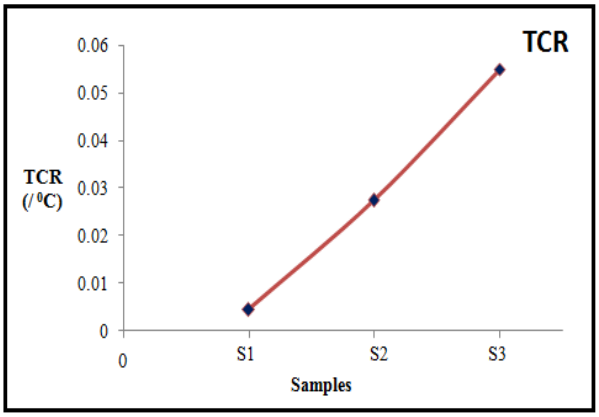

Fig. 4 TCR of nanocrystalline ZnO thin films

The temperature coefficient of resistance was -0.00447 /^{0} C and -0.02743 /^{0} C, -0.05486 to S1, S2 and S3 samples respectively. TCR was found maximum to sample S3. TCR of nanocrystalline ZnO thin film obtained negative for all samples, the negative sign indicating semiconducting behavior of the film. Figure 4 shows the variation of TCR with ZnO thin films samples. It is found that TCR is negative and its value increased gradually with increase of annealing temperature, this indicate an electron emission process which always grown with increase in annealing temperature.

Table 1 Summary of resistivity, activation energy and TCR for nanocrystalline ZnO thin films.

Thin film Samples	Resistivity (Ω-cm)	Activation Energy (eV)		TCR /^{0} C
		Low temperature	High temperature	
S1	1.8×10^{-4}	0.48194	0.27090	-0.00447
S2	5.6×10^{-3}	0.56973	0.38601	-0.02743
S3	3.6×10^{-1}	0.66386	0.39289	-0.05486

Structural characterization:

FESEM

ZnO thin films prepared by thermal evaporated technique were observed to be non porous as per FESEM analysis as shown in Figure 5 (a), (b) and (c).

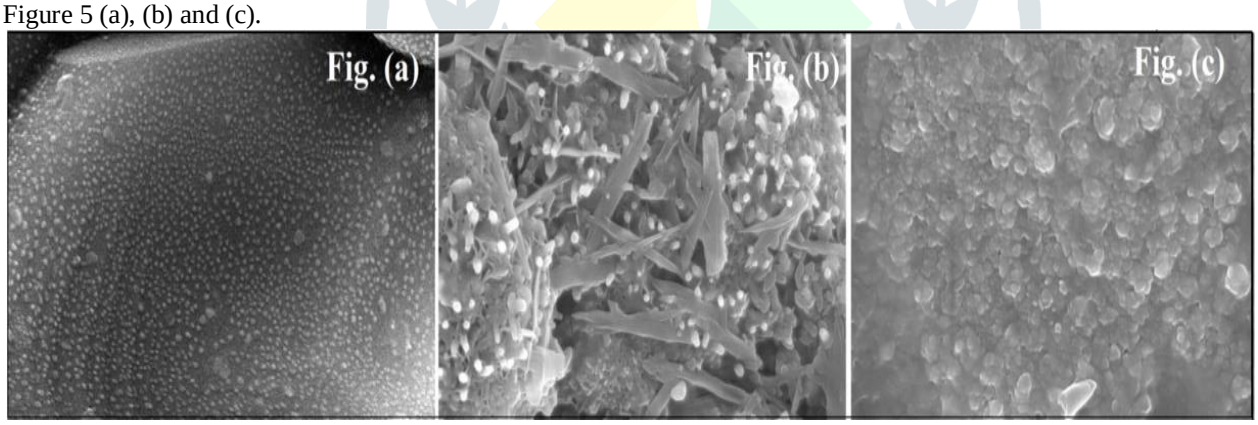

Fig. 5 (a) FESEM of un-annealed, (b) and (c) annealed thin films.

The average particle size of films was calculated by using image J software for spherical particles. The average particle size of ZnO thin films at sample S1, S2 and S3 were found 483 nm, 376 nm and 204 nm respectively.

EDAX

The EDAX result shows variation of Zn and O with un-annealed and annealed of ZnO thin films. From the EDAX spectra, it is found that mass % and atomic wt. % of Zn and O is nearly matched. As per Energy dispersive analysis by x-ray spectra, the sample S3 has more oxygen excess. It was found that ZnO thin films are non-stoichiometric. Table 2 gives quantitative elemental analysis of all samples. This excess oxygen might have been adsorbed during annealing of films.

XRD

The XRD patterns shown in Figure 6 are used to study of crystal structure of prepared un-annealied and annealied ZnO thin films samples. Sample S1 shows poor peaks but sample S2 and S3 are shows more peaks with increase annealing temperature. The S1 sample shows lower diffraction peak intensities compared to S2 and S3 samples. The peaks intensities increase with the rise annealing temperatures. From XRD pattern observed that diffraction peaks corresponds to the Wurtzite hexagonal nanocrystalline structure of ZnO (JCPDS card No. -06454).It has been observed that the optimum peak at 34.836 indicates that [002] for S3 samples. The maximum peak intensities of an XRD pattern because of the better crystallinity for sample S3. As per structural analysis the grain size were calculated by using Scherrer formula. The grain size of thin film samples S1, S2 and S3 were found 86 nm, 71 nm and 52 nm respectively. As per results grain size found minimum to Sample S3.

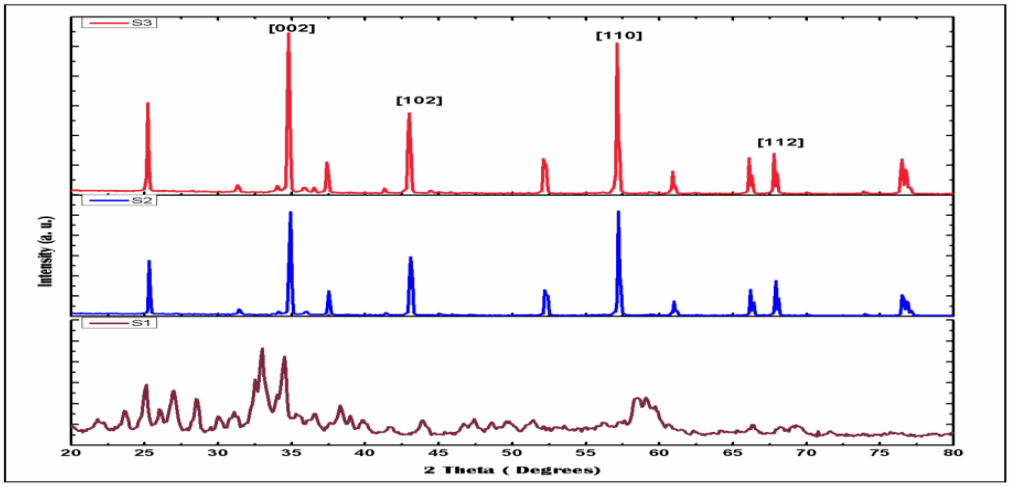

Fig. 6 (a) XRD pattern of un-annealed, (b) and (c) annealed thin films.

Table 2 Summary of crystallite (grain) size, average particle size, atomic elemental analysis and specific surface area from SEM, EDAX and XRD data of ZnO thin films.

Crystallite (grain) size, D nm **(XRD)**	Average particle size, d nm **(FESEM)**	Atomic % **(EDAX)**	
		Zn	**O**
86	483	64.38	35.62
71	376	54.94	45.06
52	204	27.67	72.33

From table 2, has been observed the grain size and average particle size was found reduced at sample S3.

Gas sensing study ZnO thin films:
Sensitivity

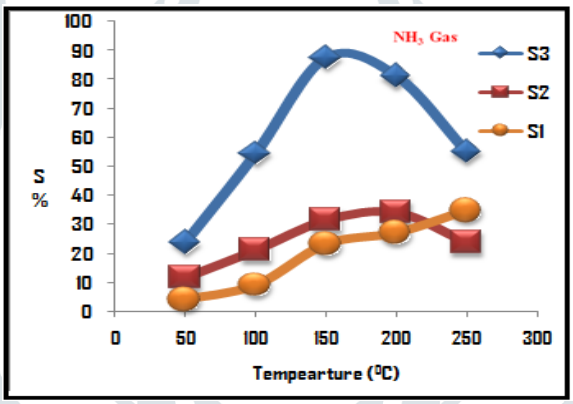

Fig. 7 Sensitivity of nanocrystalline ZnO thin films

The nanocrystalline ZnO thin film was exposed to various concentrations of NH_3 gas. NH_3 gas concentrations 50, 100, 150, 200 and 250 in PPM were used. The sample S3 showed maximum sensitivity 87.47 % at operating temperature 150^0C and gas concentration was at 100 ppm. The un-annealed sample S1 shows lower sensitivity as compare to samples S2 and S3.

PPM verses Sensitivity

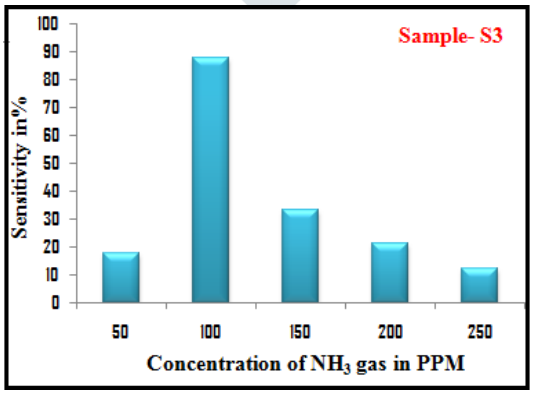

Fig.8 Sensitivity verses NH_3 gas concentration in PPM.

Figure 8 shows the variation in sensitivity for nanocrystalline ZnO thin film to different concentrations of ammonia gas. The maximum sensitivity recorded at 100 PPM. It also observed that as ppm of ammonia gas increases sensitivity decreases.

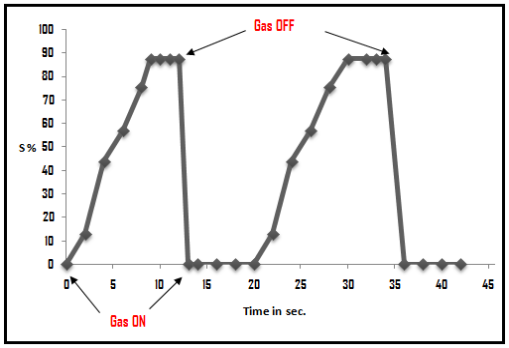

Fig. 9 Response and recovery time of nanocrystalline ZnO thin film for NH_3 gas.

Figure 9 shows the response time of nanocrystalline thin film was (~ 09 sec) while the recovery time was fast (~ 12 sec) for NH_3 gas.

NH_3 gas sensing mechanism for nanocrystalline ZnO thin film

Dwivedi et al, Madhusoodanan (2015) and Andre (2018) reported the gas sensing mechanism of ZnO sensing material to ammonia gas. The change in value of resistance in gas atmosphere is the key point of metal oxide semiconductor (MOS) sensor. The value of resistance may be increase or decrease. Resistance of the thin film depends on the nature of gas (oxidizing or reducing), type of sensing material (n type or p type) and chemical reaction (adsorption and desorption) of oxygen on the surface of sensing material. ZnO is n type metal oxide semiconductor. The NH_3 gas interacts with the surface of the ZnO thin film oxygen ions adsorbed on surface, which results in a change in resistance of the thin film. This change in resistance indicates the gas response of the film.

CONCLUSIONS

Nanocrystalline ZnO thin film could be prepared by physical vapour deposition technique on alumina substrate. The structural characteristics confirmed that the developed ZnO thin films are nanostructured in nature. The elemental analysis shows nonstoichiometric nature of films. The sample S3 of ZnO thin film was maximum sensitivity to NH_3 gas at operating temperature 150^0C and gas concentration was at 100 ppm, because high resistivity and more TCR. It has been notice that increasing annealing temperature influences the electrical and structural properties of thin films. The changes in properties of thin film were useful to enhanced gas response. Response and recovery time is also found very fast in seconds.

ACKNOWLEDGMENT

The authors thank to Department of Physics, N.H. College, Bramhapuri, Dist. Gadchiroli, India for providing me lobrotary facilities. Author also thanks to Department of Physics, Savitribai Phule Pune University, Pune for provided the facilities for SEM, EDAX and XRD characterization for current research work.

REFERENCES

[1] Baptista, A., Silva, F.J.G., Porteiro, J., Míguez, J.L., Pinto, G. and Fernandes, L., 2018. On the physical vapour deposition (PVD): evolution of magnetron sputtering processes for industrial applications. Procedia Manufacturing, 17:746-757.

[2] Fujihara, S., Ogawa, Y. and Kasai, A., 2004. Tunable visible photoluminescence from ZnO thin films through Mg-doping and annealing. *Chemistry of materials*, *16*(15), pp.2965-2968.

[3] Perrin, J., Schmitt, J., Hollenstein, C., Howling, A. and Sansonnens, L., 2000. The physics of plasma-enhanced chemical vapour deposition for large-area coating: industrial application to flat panel displays and solar cells. Plasma Physics and Controlled Fusion, 42(12B): B353.

[4] Shahidi, S., Moazzenchi, B. and Ghoranneviss, M., 2015. A review-application of physical vapor deposition (PVD) and related methods in the textile industry. The European Physical Journal Applied Physics, 71(3): 31302.

[5] Yoke Khin Yap and Dongyan Zhang., 2015. Physical Vapor Deposition. Springer Science+Business Media Dordrecht,B. Bhushan (ed.), Encyclopedia of Nanotechnology, DOI 10.1007/978-94-007-6178-0_362-3

[6] Becker, T., Ahlers, S., Braunmühl, C.B.V., Müller, G. and Kiesewetter, O., 2001. Gas sensing properties of thin-and thick-film tin-oxide materials. Sensors and Actuators B: Chemical, 77(1-2), pp.55-61.

[7] Corkery, G., Ward, S., Kenny, C. and Hemmingway, P., 2013. Monitoring environmental parameters in poultry production facilities. In Computer Aided Process Engineering-CAPE Forum 2013, 2013. Institute for Process and Particle Engineering, Graz University of Technology, Austria.

[8] Andre, R.S., Kwak, D., Dong, Q., Zhong, W., Correa, D.S., Mattoso, L.H. and Lei, Y., 2018. Sensitive and selective NH3 monitoring at room temperature using ZnO ceramic nanofibers decorated with poly (styrene sulfonate). Sensors, 18(4):1058.

[9] Gao, L., Li, Q., Song, Z. and Wang, J., 2000. Preparation of nano-scale titania thick film and its oxygen sensitivity. Sensors and Actuators B: Chemical, 71(3), pp.179-183.

[10] Scarminio, J., Lourenco, A. and Gorenstein, A., 1997. Electrochromism and photochromism in amorphous molybdenum oxide films. Thin Solid Films, 302(1-2), pp.66-70.

[11] Rahman, K.A., Schneider, S.C. and Seitz, M.A., 1997. Hopping and Ionic Conduction in Tin Oxide-Based Thick Film Resistor Compositions. Journal of the American Ceramic Society, 80(5), pp.1198-1202.

[12] Zaier, A., Meftah, A., Jaber, A.Y., Abdelaziz, A.A. and Aida, M.S., 2015. Annealing effects on the structural, electrical and optical properties of ZnO thin films prepared by thermal evaporation technique. Journal of King Saud University-Science, 27(4):356-360.

[13] Bouhssira, N., Abed, S., Tomasella, E., Cellier, J., Mosbah, A., Aida, M.S. and Jacquet, M., 2006. Influence of annealing temperature on the properties of ZnO thin films deposited by thermal evaporation. Applied Surface Science, 252(15):5594-5597.

[14] Asghar, M., Noor, H., Awan, M.S., Naseem, S. and Hasan, M.A., 2008. Post-annealing modification in structural properties of ZnO thin films on p-type Si substrate deposited by evaporation. Materials science in semiconductor processing, 11(1):30-35.

[15] Dwivedi, M., Sharma, A., Bhargava, J., Vyas, V. and Eranna, G., 2015. Detection of NH3 Using ZnO Thin Film Sensor Deposited on Si/SiO2 Substrate Derived by RF Magnetron Sputtering. Sensor Letters, 13(7):618-624.

[16] Madhusoodanan, K.N., Vimalkumar, T.V. and Vijayakumar, K.P., 2015. Gas sensing application of nanocrystalline zinc oxide thin films prepared by spray pyrolysis. Bulletin of Materials Science, 38(3):583-591.